Supporting Information

Shear-Induced Mechanochemistry: Pushing Molecules Around

Heather L. Adams[1], Michael Garvey[1], Uma Shantini Ramasamy[2], Zhijiang Ye [2], Ashlie Martini[2], Wilfred T Tysoe[1]*

[1] *Department of Chemistry and Laboratory for Surface Studies, University of Wisconsin-Milwaukee, Milwaukee, WI 53211, USA*

[2] *School of Engineering, University of California Merced, Merced CA 95343*

Table of Contents

1 Control Experiments

Control experiments were performed to ensure that the methane formed during rubbing evolved from the sliding contact and was not due to desorption from other moving parts of the vacuum chamber. In the first experiment, a thiolate-saturated copper sample was heated to 450 K to thermally decompose the thiolate species.[S1] The relatively short heating time of ~30 s ensured that only the sample and no other parts of the apparatus were heated. No methane was detected after this procedure while rubbing, indicating that the methane detected for the methyl thiolate-covered surface is due to adsorbed methyl thiolate decomposition. Second, a thiolate-saturated sample was rubbed in both directions (towards and away from the mass spectrometer). The resulting plot of 16 amu (methane) signal as a function of the number of passes, with a normal load on 0.44 N and a sliding speed of 4×10^{-3} m/s is displayed in Figure S1A. This no longer shows the exponential decrease in pulse height as a function of the number of scans, but relatively larger signals when the pin slides away from the mass spectrometer than towards it. This confirms that the methane evolves from the sliding contact rather than being due to outgassing of other moving parts of the vacuum chamber since the latter would not depend on the sliding direction. This result also indicates that methane evolved from the rear of the contact as methane formed within the contact is released. Similar trapping of shear-induced reaction products has been found in MD simulations.[S2] An expanded methane desorption pulse is shown in Figure S1B, which indicates that methane is only detected while rubbing.

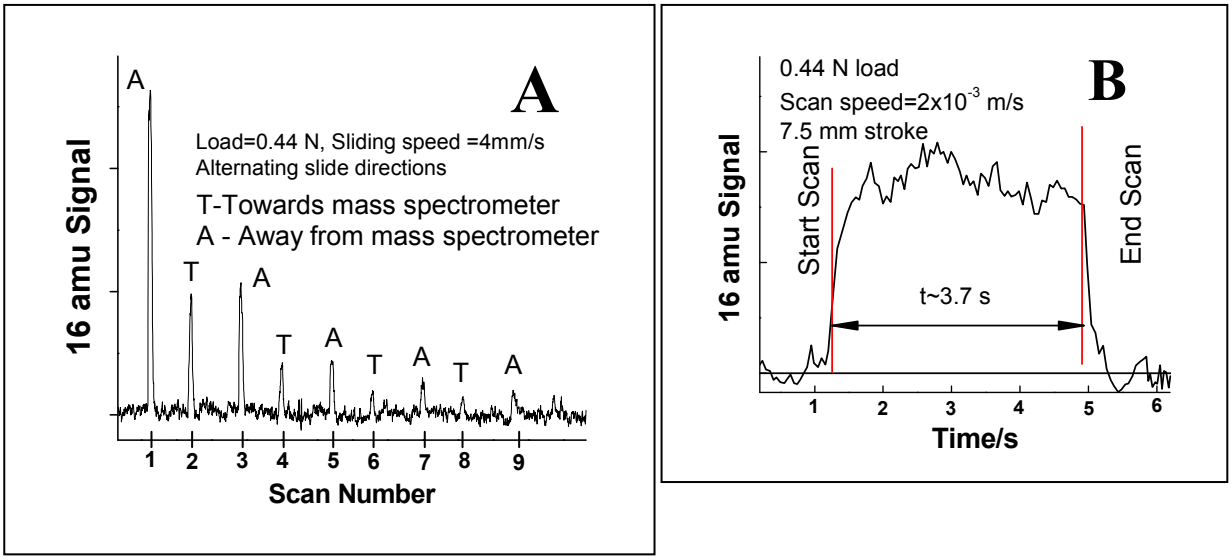

Figure S1. (**A**) Plot of the 16 amu (methane) signal measured during reciprocating sliding on a thiolate-saturated copper foil as a function of the number of scans at a sliding speed of 4×10^{-3} m/s with a normal load of 0.44 N. The methane signals measured while the pin is moving towards the sample are labeled T and those measured with the pin moving away from the sample are labeled A. (**B**) Expanded profile of a methane desorption pulse measured at a sliding speed of 2×10^{-3} m/s with a normal load of 0.44 N.

2 Analysis of Shear-Induced Desorption Kinetics

For a first-order reaction with a shear force F, $k(F)$, the rate of change of surface coverage θ due to mechanochemical desorption is:

$$-\frac{d\theta}{dt} = k(F)\theta \tag{S1}$$

Defining the coverage at the inlet of the contact as θ_I, and the coverage at the outlet as θ_O as the contact slides over a portion of an adsorbate-covered wear track, the decrease in coverage $\Delta\theta = \theta_I - \theta_0$ is given by:

$$\theta_O = \theta_I \exp(-k(F)t_C) \tag{S2}$$

so that $\Delta\theta = \theta_I(1-\exp(-k(F)t_C))$ where t_C is the contact time. The decrease in thiolate coverage results in gas-phase methane formation so that the methane yield Y, measured from the integrated area under the methane desorption pulse, is proportional to $\Delta\theta$ so that

$Y = A\theta_I(1-\exp(-k(F)t_C))$, where A is a normalization constant. The inlet thiolate coverage for the first pass $\theta_I(1) = 1$ so that the methane desorption yield during the first pass is $Y_1 = A(1-\exp(-k(F)t_C))$. The inlet coverage for the second pass, $\theta_I(2)$ equals the outlet coverage for the first pass; $\theta_I(2) = \exp(-k(F)t_C)$. Thus, the desorption yield in the second pass is given by: $Y_2 = A\exp(-k(F)t_C)(1-\exp(-k(F)t_C)$. Repeating this process shows that the yield for the n^{th} pass, defined as the total amount of methane produced in each pass, is given by:

$$Y_n = A(1-\exp(-k(F)t_C))\exp(-(n-1)k(F)t_C) \tag{S3}$$

The sum over all yields should be the initial coverage (unity). Putting $\alpha = \exp(-k(F)t_C)$ gives $Y_n = A(1-\alpha)\alpha^{(n-1)}$. The total yield Y_{tot} is obtained by summing over all values of n:

$$Y_{tot} = A(1-\alpha)\sum_{n=1}^{\infty}\alpha^{(n-1)} \tag{S4}$$

Since α is less than unity, the series converges giving $Y_{tot} = A = 1$ leading to an equation for Y_n:

$$Y_n = (1-\alpha)\alpha^{(n-1)} \tag{S5}$$

and yields an equation that depends on $k(F)t_C$ for a first-order reaction.

3 Mechanics of a Ball in a Groove

Experiments were carried by initially forming a wear track (100 ± 10 μm wide), on the clean copper surface for ~50 scans, and the track width does not increase with additional rubbing. While this is not expected to form an atomically flat surface, an atomic force microscope image of the wear track region (Figure S2), shows that shallow grooves are formed along the sliding direction on an otherwise rather flat surface. The surface has a root mean square roughness of ~

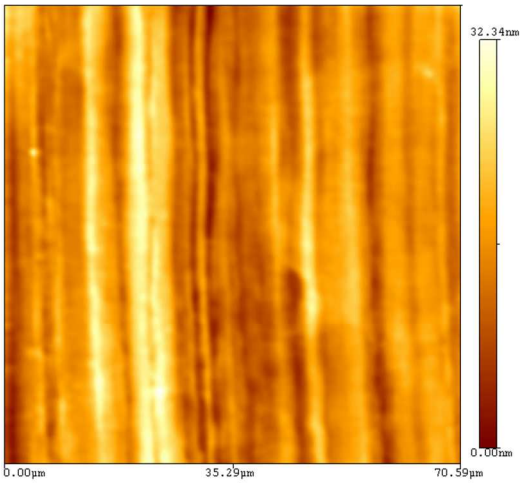

Figure S2: Atomic force microscope image of a 70 μm × 70 μm region of the wear track region after completion of the run-in period.

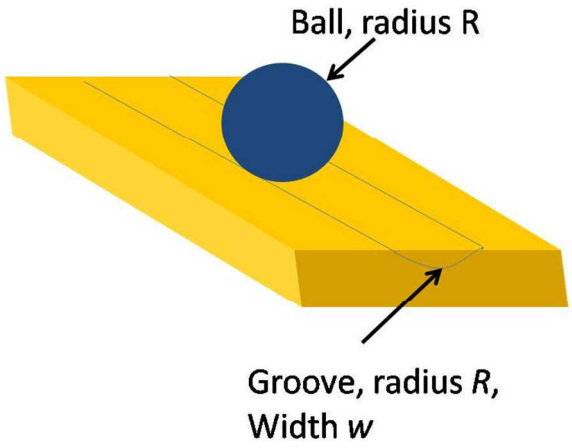

Figure S3: Diagram showing the geometry of a spherical contact in a groove formed during the run-in period.

5 ± 1 nm. An analysis of the contact area is thus initially carried out for an elastic contact for a ball of radius *R* sliding in a groove as illustrated in Figure S3. Such an elastic contact will provide an upper limit for the contact area. This result is compared with a calculation which assumes that the interface deforms completely plastically to provide a lower limit for the contact area.

3.1 Conformal Elastic Contact

The shear-induced reaction occurs on a wear track formed by rubbing the tungsten carbide pin against a copper surface. This results in a constant friction coefficient and a stable wear track, so that the contact between the pin and resulting groove may deform elastically. In order to establish an elastic contact model, we calculate the values of *A* and *B* (equations 4.4 and 4.5 and Appendix 2 in Johnson's book [S3]) for two objects that have principal radii of curvature *R'* and *R"* from:

$$(A+B)=\frac{1}{2}\left(\frac{1}{R'_1}+\frac{1}{R''_1}+\frac{1}{R'_2}+\frac{1}{R''_2}\right) \tag{S6}$$

$$|B-A|=\frac{1}{2}\left\{\left(\frac{1}{R'_1}-\frac{1}{R''_1}\right)^2+\left(\frac{1}{R'_2}-\frac{1}{R''_2}\right)^2+2\left(\frac{1}{R'_1}-\frac{1}{R''_1}\right)\left(\frac{1}{R'_2}-\frac{1}{R''_2}\right)cos2\alpha\right\}^{1/2} \tag{S7}$$

where the subscripts *1* and *2* label the two contacting objects. The resulting elastic displacement is given by (Equation 4.7 [S3]):

$$\bar{u}_{z1}+\bar{u}_{z2}=\delta-Ax^2-By^2 \tag{S8}$$

and can be used to calculate the form of the contact mechanics. Two cases are considered. In the first, it is assumed that the groove has the same radius *R* as the tungsten carbide ball (see Figure S3). Taking the pin as object *1* and the groove as object *2* gives: Tip (Object 1): $R'_1 = R''_1 = R$; Groove (Object 2): $R'_2 = -R, R''_2 = \infty$

Thus: $A+B=\frac{1}{2R}$ and $|B-A|=\frac{1}{2R}$ so that:

$$\bar{u}_{z1}+\bar{u}_{z2}=\delta-\frac{1}{2R}y^2 \tag{S9}$$

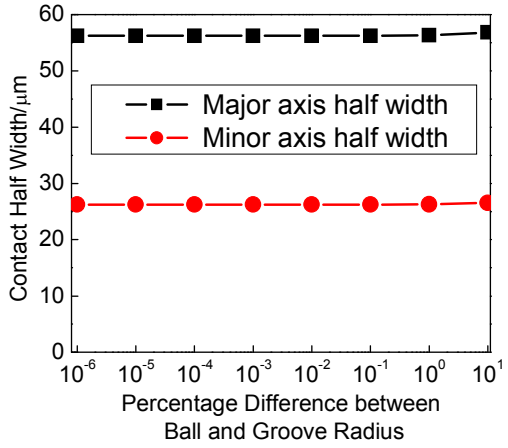

Figure S4: Plot of the major and minor axis half-widths for an elliptical contact of a spherical ball on a groove with a radius slightly larger than that of the ball, plotted against the percentage difference between the ball and groove radius.

This is the form of the displacement for a line contact of a cylinder of radius r_1 in parallel contact with a cylinder of radius r_2 (section c, Page 99, Johnson), where $\frac{1}{R} = \left(\frac{1}{r_1} + \frac{1}{r_2}\right)$, if one of the cylinders corresponds to a flat surface ($r_1 = \infty$) and the other cylinder to with a radius $r_2 = R$. This yields the width of the contact region $2a$ as:

$$a^2 = \frac{4PR}{\pi E^*} \qquad \text{(S10)}$$

where P is the load per unit length, R the ball (and wear track) radius. If the load is L (0.44 N in our experiment), and w is the width of the wear track (100 ± 10 μm), the value of a can be calculated. Using the mechanical properties in Table S1 gives $E^* = 1.06\times10^{11}$ Pa where E* is given by: $\frac{1}{E^*} = \frac{1-\nu_1^2}{E_1} + \frac{1+\nu_2^2}{E_2}$, where the subscripts label the two contacting bodies, and E is the elastic modulus and ν the Poisson's ratio. Now, $P = \frac{L}{w} = 4400 \pm 400$ N/m, so that the width of the contact ($2a$) = 37 ± 2 μm. The average contact pressure P_C can be calculated as $\frac{L}{2aw}$ and yields a value of 120 ± 6 MPa.

3.2. Elastic Contact with Different Ball and Groove Radii

Alternatively, if the groove radius is slightly larger than the ball radius, the above calculation yields an elliptical contact. For this analysis, we use the general equations for elliptical contact

between two elastic bodies. [S4] The major and minor half widths of the ellipse are $a = k_1\left(\frac{3LR'}{E^*}\right)^{1/3}$ and $b = k_2\left(\frac{3LR'}{E^*}\right)^{1/3}$, respectively, where *R'* is the reduced radius of curvature and k_1 and k_2 are contact coefficients. In this case, the radius of the groove is not accurately known, so that the reduced radius of curvature is calculated assuming a range of groove radii, up to a value of 10% larger than the ball radius. The result is shown in Figure S4, which reveals that the values of the major half axes do not vary significantly with the groove radii, yielding a value of *a*, the major half axis width of ~65 μm, and *b*, the minor half axis width of ~26 μm. This results in an average contact length perpendicular to the sliding direction of ~40 μm and, using $P_c = \left(\frac{L}{\pi ab}\right)$, an average pressure of ~95 MPa.

	Elastic modulus, *E* /Pa	Poisson ratio, *v*
Copper	1.17×10^{11}	0.335
Tungsten carbide	5.0×10^{11}	0.24

Table S1. Parameters used for the calculation of a tungsten carbide ball against a wear track on a copper substrate.[S5]

3.3 Plastic Contact

The Knoop hardness of the annealed copper foil has been measured to be ~450 MPa [S6] so that the contact width calculated by assuming that the surface deforms plastically is ~10 μm. This value is reasonable since the width calculated in sections S3.1 and S3.2 for an elastic contact lies between the maximum possible value (the width of the wear track, ~100 μm) and this minimum value.

4 Calculation of Surface Temperature During Sliding

Since an elastic contact is formed after the run-in period during the shear-induced desorption experiment, the maximum flash temperature rise is first calculated for a rectangular contact of area ($2aw$) of 3.7×10^{-9} m^2 calculated in the previous section. For a sliding velocity U of 4 mm/s at a normal load of 0.44 N and a friction coefficient of 0.52, the rate of heat supply per unit area $q = 2.47\times10^5$ W/m^2. This is an upper limit since the friction is reduced by the presence of the thiolate species. The parameters for the copper substrate and tungsten carbide ball used for the temperature rise calculation are summarized in Table S2.

	Copper	Tungsten carbide
K, Thermal conductivity (W/m/K)	401	65
ρ, Density (kg/m^3)	8933	1.56×10^4
C_P, Specific heat (J/kg/K)	390	200
k, Thermal diffusivity (m^2/s)	1.15×10^{-4}	2.08×10^{-5}
P_e, Peclet number	3.21×10^{-4}	1.78×10^{-3}

Table S2: Parameters used in the surface temperature calculation during sliding.[S5]

The maximum temperature rise during sliding for low Peclet numbers (below 0.1) is given by: $T_f = \frac{4kq}{\pi KU}(P_e \ln(P_e) - 1.116P_e)$.[S7] This yields a maximum temperature rise for copper of 6.7×10^{-2} K and for tungsten carbide of 0.34 K. It has been shown that this analysis gives good agreement with more complete solutions.[S8] An analysis of the temperature rise for more severe plastic deformation in the contact [S9] gives $T_f = 4.43\times10^3 \frac{\mu U}{K}$ yielding a temperature rise of 0.23 K. Comparison with a more complete finite-element analysis of the temperature rise shows that this equation is accurate to about 26%.[S10] Thus, the interfacial temperature rise is much less than 1 K. In order for the measured shear-induced rate constant during rubbing to be due to an

interfacial temperature increase, T_f would have to be ~170 K, about 500 times larger than the highest calculated temperature increase.

5 Simulation Details

5.1Empirical Model of Bonded and Non-Bonded Interactions

The Polymer Consistent Force Field (PCFF) with a global cutoff of 1.0 nm was used to describe bond, angle, torsion, and out-of-plane interactions between all atoms. Bond interactions are described by $E = K_2(r - r_0)^2 + K_3(r - r_0)^3 + K_4(r - r_0)^4$ where E is energy, r is distance, and r_0, K_2, K_3, and K_4 are coefficients. PCFF is not a reactive potential, so that the bonds cannot break. Instead the form of the equation is harmonic such that the force is zero when the bonds are at their equilibrium lengths and then increases rapidly when the bonds are stretched or compressed. The interactions between two contact surface atoms are captured by the Lennard-Jones potential, $E = 4\varepsilon\left[\left(\frac{\sigma}{r}\right)^{12} - \left(\frac{\sigma}{r}\right)^{6}\right]$ where E is energy, r is distance, ε is the depth of the potential well and σ is the distance at which potential is zero.

5.2 Shear Force per Molecule

The shear force per molecule is estimated as the x-direction force on the bond between the sulfur and carbon atoms. This value is calculated based on the following equation:

$$d = \sqrt{(x_1 - x_2)^2 + (y_1 - y_2)^2 + (z_1 - z_2)^2}$$

$$f_{x-bond} = f_{total-bond}\left|\frac{(x_2 - x_1)}{d}\right| \quad \text{(S11)}$$

where d is distance, x, y, z are coordinates of atom *1* (sulfur) and *2* (carbon), $f_{x\text{-}bond}$ is the x-directional bond force, and $f_{total\text{-}bond}$ is the total bond force (per the empirical potential described in the previous section). Since there are many sulfur-carbon bonds in the simulation, there is a

distribution of bond forces at any given time. The average shear force per molecule is estimated as the mean of the *x*-direction bond-force distribution. We confirm that the simulation has converged by ensuring that the time-dependent average shear force per molecule is constant (Figure S5).

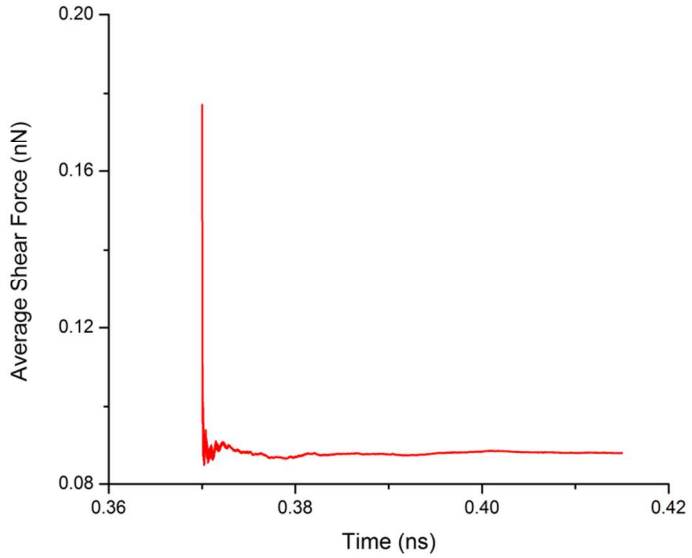

Figure S5: Time-dependent average shear force per moleculefrom a simulation at a sliding speed of 4mm/s with a contact pressure of 450 MPa.

5.3 Contact Force Distributions and Contact Pressure

The contact pressure is calculated from the net normal force acting on the top copper plate divided by the contact area. We also partially validate the simulations by analyzing the distribution of the normal and shear forces on the plates. This is calculated from the non-bonded (Lennard-Jones) force between the carbon atoms on the top plate and the carbon atoms on the bottom plate. Figure S6 shows the contact force distributions in the loading (normal) and sliding (shear) directions. These distributions are obtained from forces output every 0.25ps during a 1

nm simulation. The results are consistent with distribution reported in a previous simulation study.[S11]

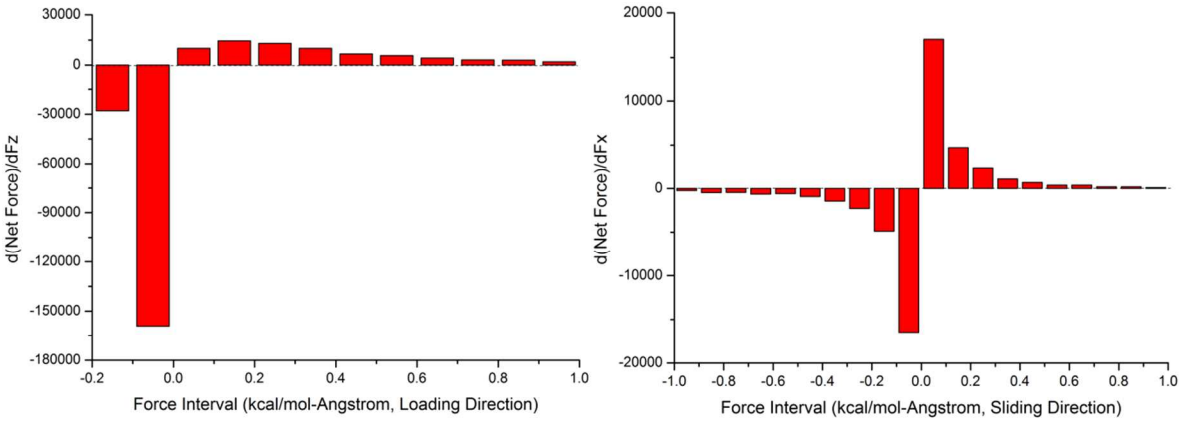

Figure S6: Contact force distributions along the loading (left figure) and sliding (right figure) directions taken at a sliding speed of 40 m/s with a contact pressure of 450 MPa.

6 Movie

An animation of the simulation is shown in Movie S1.

7 References

S1. Furlong, O.J.; Miller, B.P.; Li Z, Walker, J, Burkholder, L.; Tysoe, W.T., The Surface Chemistry of Dimethyl Disulfide on Copper. *Langmuir* **2010**, *26,* 16375-16380.

S2. Harrison, J.A.; Brenner, D.W., Simulated Tribochemistry - An Atomic Scale View of the Wear of Diamond. *J. Am. Chem. Soc.* **1994,** *116,* 10399-10402.

S3. Johnson, K.L., Contact mechanics. 1985 Cambridge University Press, Cambridge, 1985.

S4. Stachowiak, G.W.; Batchelor, A.W., *Engineering Tribology*. Elsevier Butterworth-Heinemann: Amsterdam; Boston, 2005.

S5. Kaye, G.W.C.; Laby, T.H., *Kaye & Laby Tables of Physical & Chemical Constants*. National Physical Laboratory: Middlessex, England, 1995.

S6. Gao, F.; Furlong, O.; Kotvis, P.V.; Tysoe, W.T.,. Pressure Dependence of Shear Strengths of Thin Films on Metal Surfaces Measured in Ultrahigh Vacuum. *Tribol. Lett.* **2008,** *31,* 99-106.

S7. Jaeger, J.C., Moving Sources of Heat and the Temperature in Sliding Contacts. *Proc Roy Soc, NSW,* **1943,** *76,* 21.

S8. Bansal, D.G.; Streator, J.L., AMethod for Obtaining the Temperature Ddistribution at the Interface of Sliding Bodies. *Wear* **2009,** *266,* 721-732.

S9. Ashby, M.F.; Abulawi, J.; Kong, H.S., Temperature Maps for Frictional Heating in Dry Sliding. *Tribol Trans* **1991,** *34,* 577-587.

S10. Smith, E.H.; Arnell, R.D., A New Approach to the Calculation of Flash Temperatures in Dry, Sliding Contacts. *Tribol. Lett.* **2013,** *52,* 407-414.

S11. Harrison, J. A.; Schall, J. D.; Knippenberg, M. T.; Gao, G.; Mikulski, P. T.; Elucidating Atomic-Scale Friction Using Molecular Dynamics and Specialized Analysis Techniques. *J. Phys.: Condens. Matter* 2008, **20**, 354009.